24 August 2012 | S10

Science

AAAS

A Periciliary Brush Promotes the Lung Health by Separating the Mucus Layer from Airway Epithelia

Brian Button,[1]* Li-Heng Cai,[2]* Camille Ehre,[1] Mehmet Kesimer,[1,3] David B. Hill,[1] John K. Sheehan,[3] Richard C. Boucher,[1]† Michael Rubinstein[2,4]†‡

Mucus clearance is the primary defense mechanism that protects airways from inhaled infectious and toxic agents. In the current gel-on-liquid mucus clearance model, a mucus gel is propelled on top of a "watery" periciliary layer surrounding the cilia. However, this model fails to explain the formation of a distinct mucus layer in health or why mucus clearance fails in disease. We propose a gel-on-brush model in which the periciliary layer is occupied by membrane-spanning mucins and mucopolysaccharides densely tethered to the airway surface. This brush prevents mucus penetration into the periciliary space and causes mucus to form a distinct layer. The relative osmotic moduli of the mucus and periciliary brush layers explain both the stability of mucus clearance in health and its failure in airway disease.

Mucus clearance in the mammalian lung has evolved to trap and clear a wide variety of inhaled toxicants and infectious agents from airway surfaces (*1*–*3*). The system consists of two components (*4*, *5*): (i) a mucus layer that traps inhaled particles and transports them out of the lung by cilia-generated forces and (ii) a periciliary layer (PCL) that provides a favorable environment for ciliary beating and cell-surface lubrication (Fig. 1A). The importance of mucus clearance is illustrated by its failure in human lung diseases, including chronic obstructive pulmonary disease (COPD) (*6*) and cystic fibrosis (CF) (*7*). Both diseases are characterized by "dehydrated" airway mucus, with mucin and globular protein concentrations several times higher than in normal mucus (*8*, *9*). Despite studies linking increased mucus concentration to the pathogenesis of airway disease—for example, via reduced rates of mucus clearance (*10*), inflammation (*11*), and infection (*12*)—quantitative models are needed to predict when mucus clearance fails and to develop therapies to treat this aspect of lung disease (*13*, *14*). A predictive airway surface clearance model requires an accurate description of the PCL structure and an understanding of the functional interactions between the PCL and the overlaying mucus layer.

On the basis of light microscopy of the airway surface (e.g., Fig. 1A) and the presumed requirement for a low-viscosity liquid layer to facilitate ciliary beating, the mucus clearance system has been represented by a two-layer gel-on-liquid model (*15*–*19*) (Fig. 1B). In this model, a "gel-like" mucus layer is propelled by cilia beating in a "watery" periciliary, that is, "sol" layer (*20*). However, the current gel-on-liquid model does not explain why there are two layers. For instance, it does not explain why the major macromolecules (*21*–*25*) of the mucus layer—MUC5AC and MUC5B, with hydrodynamic radii of ~150 to 200 nm (*26*, *27*)—do not penetrate into the ~200-nm interciliary space to form a single layer. In fact, this 200-nm interciliary space is impenetrable even to objects substantially smaller than mucins, including fluorescent beads with diameter of 40 nm (Fig. 1, C and D). It has been proposed that impenetrability of the interciliary space is due to the thixotropic actions of beating cilia (*15*, *28*). However, our observation that 40-nm particles are also excluded from the PCL when cilia beating was arrested argues against this explanation (Fig. 1E). Collectively, these data demonstrate that the gel-on-liquid model of a two-layered airway surface is qualitatively incorrect.

Gel-on-brush model of the airway surface. We propose an alternative gel-on-brush model of the mucus clearance system. In this model, the PCL is occupied by membrane-spanning mucins and large mucopolysaccharides that are tethered to cilia, microvilli, and epithelial surface (Fig. 2A) (*29*). We postulate that these tethered

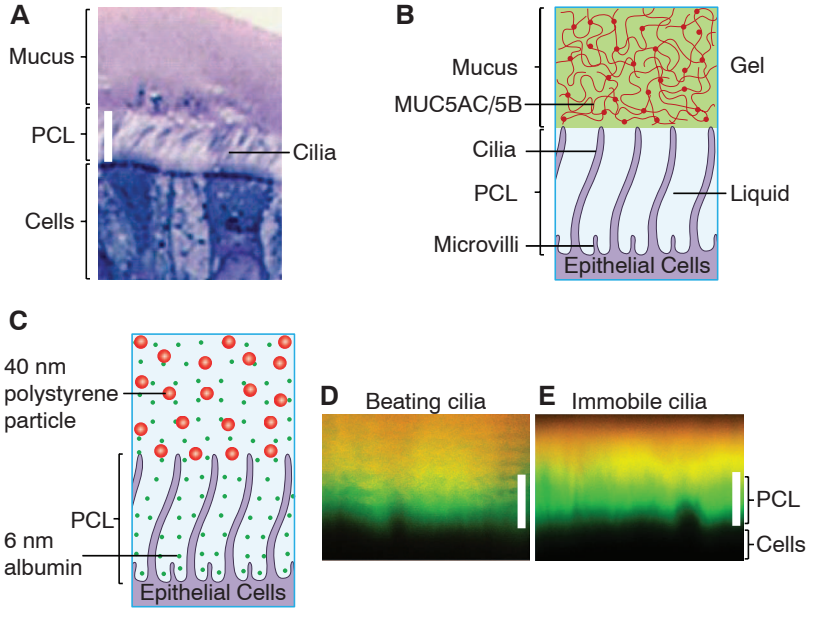

Fig. 1. The PCL is not a simple liquid layer. (**A**) Light microscopy view of the airway surface layer, comprising the mucus layer and the PCL, from fixed human bronchial epithelial cultures stained with Richardson's (*42*). Scale bar indicates 7 μm. (**B**) Schematic representation of the traditional gel-on-liquid model showing a mucus layer (comprised of gel-forming mucins, MUC5AC and MUC5B) and the PCL as a liquid-filled domain. (**C**) Schematic illustration showing penetration of small [$d \approx 6$ nm (*43*)] fluorescently labeled albumin (green) into the PCL, whereas 40-nm polystyrene particles (red) are completely excluded from the PCL. The experiments were performed after thorough washings that remove mucus, leaving solely the clean PCL, to avoid possible trapping of these particles by the mucus (*44*, *45*). (**D** and **E**) Representative XZ confocal images of well-differentiated HBE cultures with (D) normally beating cilia and (E) paralyzed, that is, immobile, cilia [pretreated for 10 min with 1% isoflurane to produce reversible ciliastasis (*46*)]. The exclusion zone (green region) was accessible to the green albumin but not the larger particles, whereas the yellow region was accessible to both. The wavy streaks in (D) are an artifact of beating cilia during image acquisition. Scale bars, 7 μm.

[1]Cystic Fibrosis Research and Treatment Center, University of North Carolina, Chapel Hill, NC 27599–7248, USA. [2]Curriculum in Applied Sciences and Engineering, University of North Carolina, Chapel Hill, NC 27599–3280, USA. [3]Department of Biochemistry and Biophysics, University of North Carolina, Chapel Hill, NC 27599–7260, USA. [4]Department of Chemistry, University of North Carolina, Chapel Hill, NC 27599–3290, USA.

*These authors contributed equally to this work.
†These authors contributed equally to this work.
‡To whom correspondence should be addressed. E-mail: mr@unc.edu

macromolecules form an extracellular brush with a sufficiently high concentration to establish a mesh that prevents both MUC5AC and MUC5B mucins in the mucus layer and inhaled particles deposited on the airway surface from penetrating the PCL. We also predict that the relatively high concentration of membrane-tethered macromolecules in this extracellular brush produces intermolecular repulsion within this layer, which stabilizes the PCL against compression by an osmotically active mucus layer. Stabilization of the PCL is required for formation of the distinct mucus layer and for effective mucus clearance. In contrast, dehydration-induced destabilization of this two-layer system produces failure of clearance. Thus, the gel-on-brush model both describes the cell biological basis of the two layers and the biophysical interactions between these layers that control mucus clearance. The following experiments test the key aspects of this new model.

Evidence for a macromolecular mesh in the PCL. By using rapid freezing techniques coupled with electron microscopy (EM), we observed an electron-dense meshwork with apparent mesh size on the order of ~20 to 40 nm in the PCL region of primary human bronchial epithelial (HBE) cell cultures (Fig. 2, B and C). Unlike the overlying mucus layer, this PCL mesh could not be extracted by vigorous washings expected to remove adherent secreted mucins. We therefore hypothesized that the PCL mesh consists of large macromolecules, such as membrane-spanning mucins [MUC1, MUC4, MUC16, and MUC20 (*29*, *30*)] and tethered mucopolysaccharides [e.g., heparan sulfate (*31*)]. Immunohistochemistry studies of freshly excised human airways identified several of these membrane-tethered macromolecules, including mucins MUC1 (Fig. 2D) and MUC4 (Fig. 2E) and heparan sulfate (not shown), attached to cilia, microvilli, and the cell surface of conducting airways.

Mesh size of the PCL. Mesh size is a parameter that describes important physical properties of polymer solutions, gels, and brushes, including their permeability to particles and macromolecules and their osmotic pressure. In polymer physics, the mesh size, called correlation length, ξ, is defined as the average distance between nearest segments of neighboring macromolecules (*32*). Images of the PCL generated from the rapid fixation and EM approach (Fig. 2, B and C) might not provide reliable values of mesh size because of fixation and staining artifacts. Therefore, a technique was developed to quantify the PCL mesh size in living HBE cultures. This technique has its basis in the partitioning concept that, as probes of size d enter the PCL layer from dilute solutions (*32*), they are repelled by crowded, tethered macromolecules within the PCL and have to pay a free energy penetration price, $F \approx k_B T(d/\xi)^\gamma$ (where $\gamma = 2$ for polymers and $\gamma = 3$ for particles, k_B is Boltzmann constant, and T is absolute temperature; supplementary text). Scaling prefactors on the order of unity have been omitted

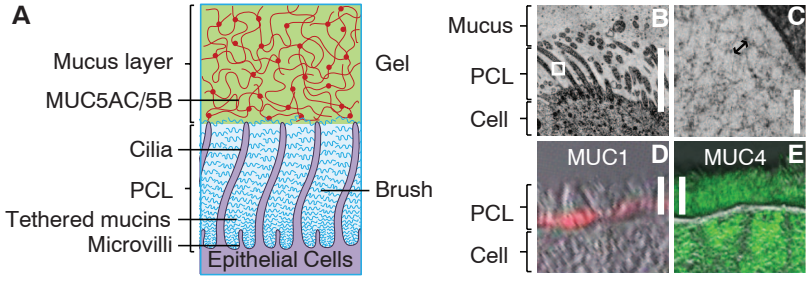

Fig. 2. Gel-on-brush model of the PCL. (**A**) Schematic representation of the gel-on-brush hypothesis of the PCL: Tethered macromolecules, such as membrane-bound mucins, form a brushlike structure of the PCL. (**B** and **C**) Morphological evidence for the gel-on-brush model is revealed by rapid freeze imaging of HBE cultures exhibiting extensive meshlike structure with mesh [depicted by the arrow in (C)] on the order of ~20 to 40 nm in the PCL. Immunological evidence showing the presence of tethered mucins on freshly excised human airway tissue: (**D**) MUC1 (red) is located at the bottom of the PCL; (**E**) MUC4 (green) spans the whole PCL. Scale bars in (B), (D), and (E), 7 μm; in (C), 100 nm. Double-headed arrow in (C) indicates 30 nm. White box in (B) denotes area of magnification depicted in (C).

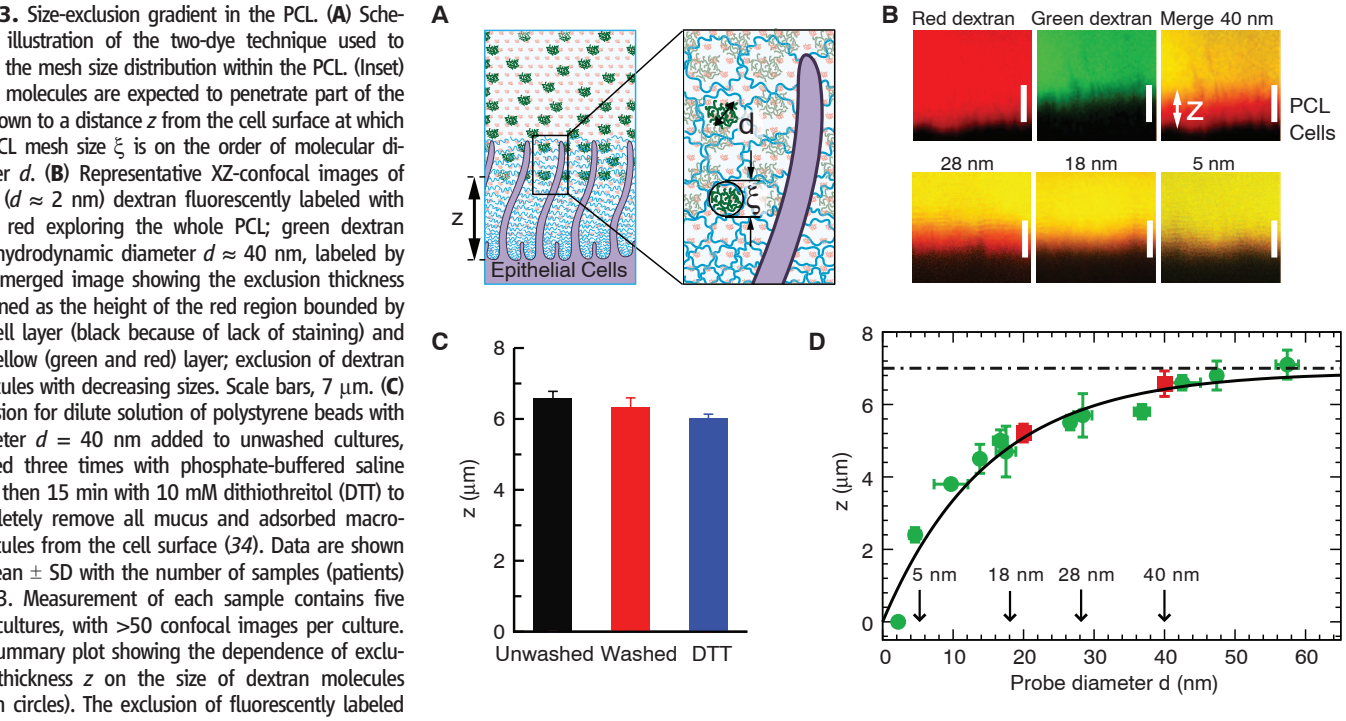

Fig. 3. Size-exclusion gradient in the PCL. (**A**) Schematic illustration of the two-dye technique used to probe the mesh size distribution within the PCL. (Inset) Probe molecules are expected to penetrate part of the PCL down to a distance z from the cell surface at which the PCL mesh size ξ is on the order of molecular diameter d. (**B**) Representative XZ-confocal images of small ($d \approx 2$ nm) dextran fluorescently labeled with Texas red exploring the whole PCL; green dextran with hydrodynamic diameter $d \approx 40$ nm, labeled by FITC; merged image showing the exclusion thickness z defined as the height of the red region bounded by the cell layer (black because of lack of staining) and the yellow (green and red) layer; exclusion of dextran molecules with decreasing sizes. Scale bars, 7 μm. (**C**) Exclusion for dilute solution of polystyrene beads with diameter $d = 40$ nm added to unwashed cultures, washed three times with phosphate-buffered saline (PBS) then 15 min with 10 mM dithiothreitol (DTT) to completely remove all mucus and adsorbed macromolecules from the cell surface (*34*). Data are shown as mean ± SD with the number of samples (patients) $n = 3$. Measurement of each sample contains five HBE cultures, with >50 confocal images per culture. (**D**) Summary plot showing the dependence of exclusion thickness z on the size of dextran molecules (green circles). The exclusion of fluorescently labeled 20- and 40-nm polystyrene particles (red squares) are added for comparison. Data points are mean ± SD ($n = 3$ to 5). Solid curve is the best fit to the data by an empirical equation $\{z(d) \approx 7\ \mu m[1 - \exp(-d/15\ nm)]\}$, and dash-dotted line at 7 μm represents the height of the outstretched cilia.

from this and following equations. The partition coefficient, $P(d)$, of probes of size d, defined as the ratio of concentration of the probes in the PCL to their concentration in the dilute solution outside the PCL, is the Boltzmann weight corresponding to this free energy penalty: $P(d) = \exp(-F/k_BT) \approx \exp\{-[d/\xi(z)]^\gamma\}$. $\xi(z)$ in this expression describes variations of mesh sizes ξ in the PCL with distance z from the cell surface. Because an exponential is a rapidly varying function, this expression can be approximated by a step function (*33*), with a simple interpretation that probe molecules or particles penetrate the PCL from dilute solutions down to the depth $z(d)$ at which the probe size (d) is equal to the mesh size (ξ) (Fig. 3A). Within this step function approximation, the depth profile of mesh sizes $z(\xi)$ is identical to the exclusion profile $z(d)$. More rigorous analyses accounting for both the exponential form of the partition coefficient and the polydispersity of probe molecules led only to a small correction in the depth profile of mesh sizes $z(\xi)$ (supplementary text, fig. S2, and table S1).

The PCL exclusion profile $z(d)$ was measured by two-color fluorescent imaging of two probes of well-defined sizes: (i) "large" green fluorescent dextran molecules of hydrodynamic diameter d and (ii) "small" red fluorescent dextran molecules. A mixture of these red and green molecules was applied in dilute solutions to HBE cultures washed free of the overlying mucus layer (Fig. 3B). The small ($d \approx 2$ nm) Texas red fluorescently labeled dextrans completely penetrated the PCL and reached the cell surface (Fig. 3B, left), as evidenced by the complete overlap of the fluorescence profile with that of a sub-nanometer dye, rhodamine 110 (fig. S4). In contrast, fractionated large green fluorescein isothiocyanate (FITC)–labeled dextran molecules with $d \approx 40$ nm were excluded from the PCL (Fig. 3B). The exclusion zone $z(d)$, defined as the part of the PCL accessible to small dextrans but not to large ones, had a height $z \approx 6.5$ μm, close to the height of outstretched cilia (Fig. 1A). The yellow region above the exclusion zone represents the region accessible to both large (green) and small (red) dextrans. The 6.5-μm exclusion zone is in agreement with the results using the 40-nm fluorescent beads (Fig. 1, C to E). This exclusion persisted after extensive washing of the cell surface in the absence or presence of a reducing agent (10 mM dithiothreitol) sufficient to remove adsorbed macromolecules, including the gel-forming mucins (*34*) (Fig. 3C). Thus, these findings confirm the main hypothesis of our gel-on-brush model that the PCL is occupied by macromolecules that are strongly tethered to the cell surface. Furthermore, these tethered macromolecules are at sufficiently high concentrations to produce a tight mesh with a

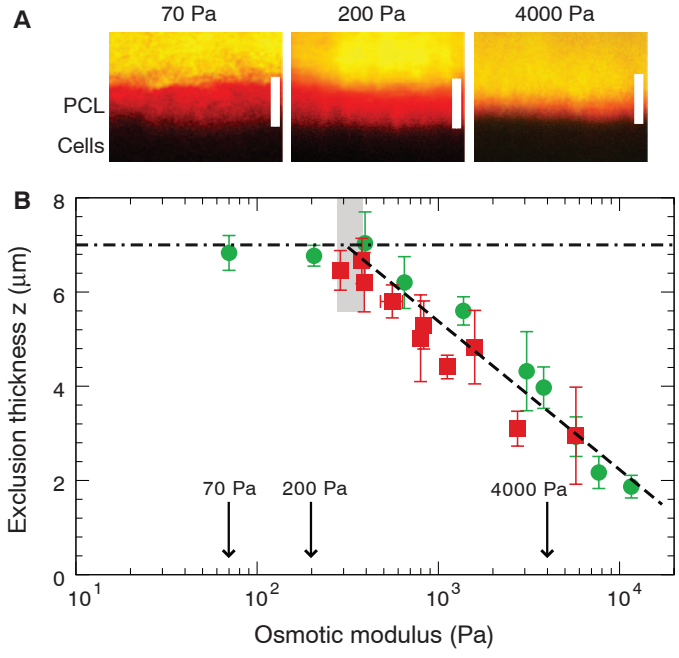

Fig. 4. Osmotic compression of the PCL brush by mucus and mucus simulants. (**A**) Representative XZ-confocal images showing progressive compression of the PCL brush by large dextran molecules ($d > 50$ nm) of increasing osmotic moduli. Scale bars, 7 μm. (**B**) Summary data of the exclusion thickness (z) of the large dextran molecules (green circles) and endogenous mucus (red squares) versus their osmotic moduli. Data points are mean ± SD ($n = 3$ to 5). Dashed black line represents the best linear fit to the dependence of PCL height on the logarithm of osmotic modulus of mucus or mucus simulants for $z < 6$ μm: $z \approx 7\ \mu m - 3.15\log(K/340\ Pa)$. The highlighted region represents the osmotic modulus of a fully hydrated (healthy) PCL, $K_0 \approx 300 \pm 60$ Pa, above which noticeable decrease of the PCL height was observed.

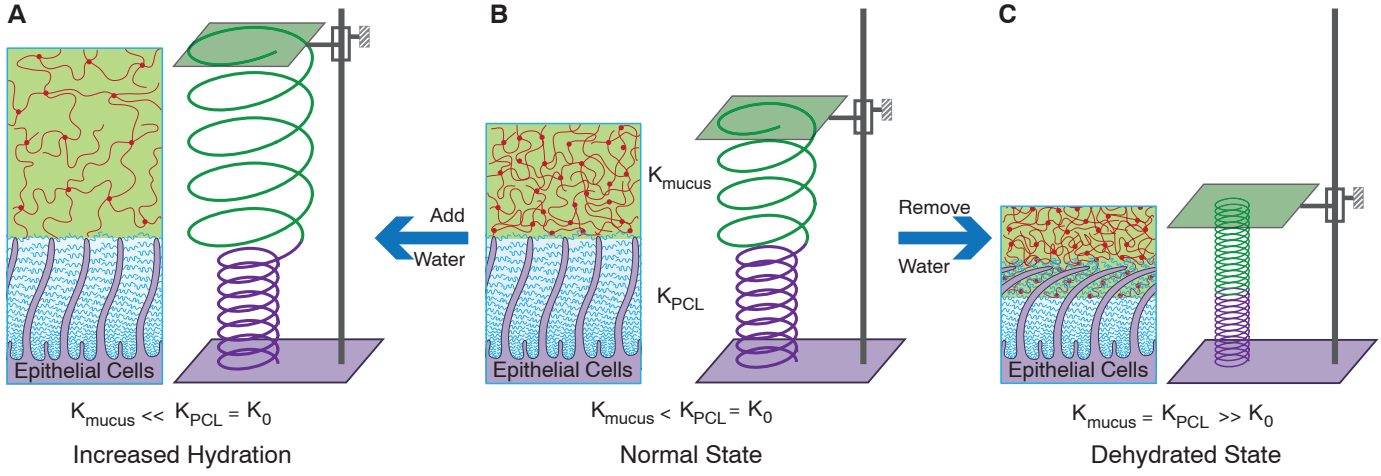

Fig. 5. (**A** to **C**) Schematic illustrations showing the effects of the relative water-drawing powers of the mucus gel and the PCL. (B) Normal state: The osmotic modulus of normal mucus is smaller than that of the PCL, represented by a green spring (K_{mucus}) with diameter larger than a purple spring ($K_{PCL} = K_0$). The volume of water in the system is depicted by the fixed distance between two plates. (A) Increased hydration: Water added to the healthy airway surface (distance between plates increased) with $K_{mucus} < K_0$ preferentially enters and thus dilutes the mucus layer, leaving the PCL unchanged. The resulting osmotic modulus of the mucus layer is much smaller than that of the PCL ($K_{mucus} << K_0$). This state is depicted by increase length and diameter of the green spring with no change in the purple spring. (C) Dehydrated state (plates close to each other): As water is removed, it first preferentially leaves the mucus gel because of its lower osmotic modulus. Further dehydration leads to removal of water from both the mucus gel and the PCL. The moduli of both layers are increased and equal, represented by smaller diameters of shortened springs. This state corresponds to diseased airways (COPD and CF).

maximum size ξ of ~40 nm (fig. S3), which prevents the 40-nm dextran and beads from penetrating the PCL (Figs. 1C and 3B).

By systematically changing the size d of the green probes and measuring their depth of penetration into the PCL, we observed variations of the exclusion thickness $z(d)$ for probes of varying size d. This variation is consistent with a PCL macromolecular mesh that becomes "tighter" toward the cell surface (Fig. 3, B and D, and fig. S5). This PCL gradient mesh likely functions as a permeability barrier to prevent small infectious agents [e.g., influenza A with $d \approx 80$ to 120 nm (*35*)] from reaching the cell surface.

Osmotic modulus of the mucus layer and PCL. In addition to forming a permeability barrier (*36*), the gel-on-brush model predicts that the densely tethered macromolecules within the PCL repel each other and thus generate an osmotic pressure that regulates the hydration of the PCL. The rate of osmotic pressure variation with polymer concentration (c) defines the osmotic modulus (K), a parameter that quantifies the hydration (water-drawing) power of the system: $K = c(\partial\pi/\partial c)$.

By using a modified osmometer (*37*) incorporating a membrane permeable to ions and small proteins, we measured the osmotic pressure and calculated the osmotic modulus of the mucus layer on HBE cultures with concentrations spanning from normal to "abnormally" high values (fig. S1). The osmotic modulus (K) of the mucus layer strongly increased with mucus concentration, from 200 Pa at normal mucus concentrations (*10*) [roughly 0.01 g/ml, which is equivalent to ~2% solids (*38*)] to 3000 to 8000 Pa for severely dehydrated (concentrated) mucus in ranges reported in CF patients [>0.07 g/ml, i.e., >8% solids (*10*, *39*)].

We measured the PCL osmotic modulus by exposing washed HBE cultures to solutions containing very large ($d > 50$ nm) PCL-impenetrable polymers of varying concentrations and, hence, osmotic moduli (Fig. 4). Similar to the PCL penetration experiments (Fig. 3), measurements of PCL osmotic moduli were performed by using a two-fluorescent-probe technique. Unlike the PCL penetration experiments, only the concentration of the large green dextrans, and hence the osmotic modulus of the test solution, was varied.

Solutions containing large dextrans with osmotic moduli lower or comparable to the modulus of normal mucus ($K \approx 200$ Pa) did not affect the height of the PCL (Fig. 4). Only when K of the dextran solution exceeded ~300 Pa did the PCL begin to be compressed, as evidenced by the decrease in the exclusion height. Therefore, 300 Pa represents the osmotic modulus of a fully hydrated (healthy) PCL (K_0) (Fig. 4B, gray zone). Exposure to a higher concentration of dextran with a $K \sim 4000$ Pa resulted in a substantial collapse of the PCL (Fig. 4).

The probe penetration experiments described above (Fig. 3) identified a gradient of mesh sizes $\xi(z)$ in the PCL, strongly suggesting that the grafting density of macromolecules tethered to cilia increases toward the cell surface. On the basis of this observation, we predicted that the repulsion between these macromolecules, and therefore the osmotic modulus of the PCL, would also increase toward the cell surface. Indeed, the exclusion zone for the probes was observed to decrease systematically as a function of the osmotic modulus K of the mucus simulants (green circles, Fig. 4B). These findings were validated by the experiments in which the PCL was compressed by endogenous mucus at various concentrations (and osmotic moduli) (red squares, Fig. 4B). Mucus with high concentrations, mimicking those found in immobile airway secretions from diseased lungs such as CF (i.e., >0.07 g/ml (*10*, *39*) with $K >$ 3000 Pa), removed sufficient water from the PCL to cause its collapse (Fig. 4).

These data suggest that the gel-on-brush model accurately describes the forces that govern hydration of airway surfaces. The model predicts that water distributes between the two airway surface layers, that is, the mucus layer and PCL, according to their relative osmotic moduli (Fig. 5). The layer with a lower osmotic modulus changes its concentration more readily than the layer with the higher osmotic modulus. This relationship is analogous to the deformation of a pair of springs connected in series (Fig. 5B). Upon deformation of the pair, the softer spring (with lower modulus) deforms more than the stiffer one. Because the PCL is a "constrained" (tethered) system, its concentration saturates upon hydration, and therefore it has a "minimal" osmotic modulus (K_0) when the PCL is fully hydrated. In contrast, the mucus layer is under no such constraint, so its osmotic modulus can become very small upon extensive hydration. As a result, liquid added to the hydrated and healthy airway surface preferentially enters the mucus layer, leaving the PCL unchanged (Fig. 5A). Conversely, when the airway surface is dehydrated, liquid is drawn first from the mucus layer, increasing its concentration and, therefore, osmotic modulus. As the osmotic modulus of the mucus layer exceeds K_0 of the PCL, water is extracted from both layers, increasing their concentrations and osmotic moduli and resulting in compression of the PCL (Fig. 5C). Thus, the gel-on-brush model posits that (i) for health, the osmotic modulus (K_0) of the PCL must be larger than that of the mucus layer (Fig. 5B) to ensure the required hydration and lubricating properties of the PCL for normal mucus clearance and (ii) in disease, strong dehydration of the airway surface produces a mucus layer osmotic

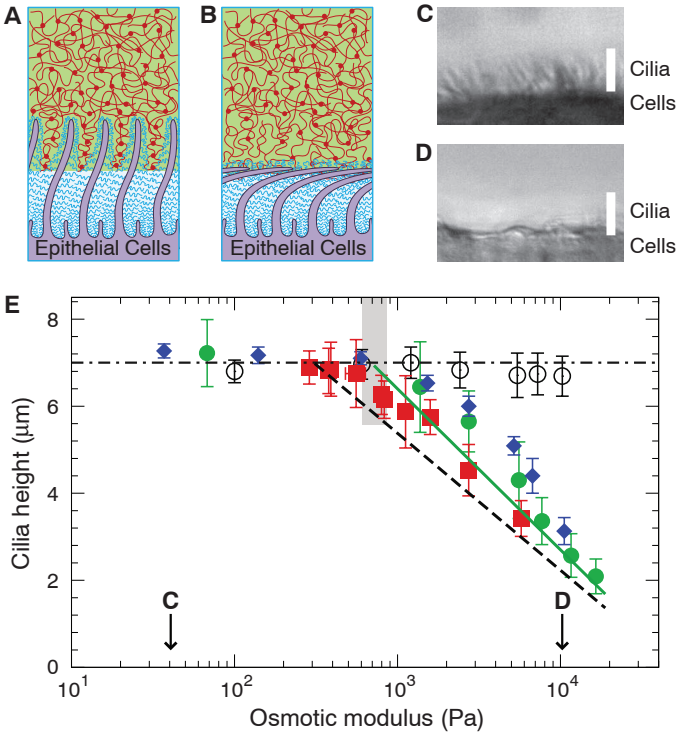

Fig. 6. Collapse of cilia by mucus and mucus simulants. Possible scenarios for the compression of the PCL brush by mucus or mucus simulants with high osmotic modulus (concentration): (**A**) tethered macromolecules are compressed toward the cilia surface without significant deformation of the cilia in comparison to the uncompressed PCL brush in Fig. 2A. (**B**) In addition to the compressed tethered macromolecules, the cilia are also deformed by solutions with high osmotic modulus. (**C** and **D**) Representative bright-field microscopy images showing the effects of low (C), ~300 Pa, and high (D), ~10,000 Pa, osmotic moduli of agarose on cilia height from HBE cultures (viewed in profile). White bars denote the length of fully extended cilia (7 μm). (**E**) Summary plot of the cilia height versus the osmotic moduli of the overlying mucus and mucus simulants, using large, PCL-impermeable dextran ($d > 50$ nm; green solid circles), low-melting point agarose ($d \approx 44$ nm; blue solid diamonds), endogenous mucus (red solid squares), and small PCL-permeable dextran ($d \approx 2$ nm; black open circles). Data points are mean ± SD ($n = 3$ to 5). PCL-permeant 2-nm dextran did not alter the height of the cilia. "C" and "D" above the x axis represent conditions illustrated above. Solid green line represents the best linear fit to the dependence of cilia height on the logarithm of osmotic modulus of mucus or mucus simulants for $K > 1000$ Pa: $z \approx 7\ \mu m - 3.33\log(K/807\ Pa)$. Dependence of the exclusion zone $z(K)$ on osmotic modulus of mucus or mucus simulants (Fig. 4B) is shown for comparison by the dashed black line. Highlighted zone represents the crossover osmotic modulus, $K_{cc} \approx 800 \pm 120$ Pa, above which noticeable decrease of the cilia height was observed.

modulus (K_{mucus}) that substantially exceeds K_0 of the healthy PCL, collapsing the PCL and slowing or abolishing mucus clearance (Fig. 5C).

There are contrasting scenarios for PCL collapse upon osmotic compression that have important implications for cilia-beating dynamics and mechanisms of mucus adhesion to the airway surface. For example, one possibility is that the tethered macromolecular brush is compressed against "extended" cilia upon exposure to dehydrated mucus or mucus simulants with high osmotic moduli, allowing penetration of mucus into the interciliary space (Fig. 6A). This scenario is expected if cilia are elastically stiffer than the surrounding brush of tethered macromolecules and dehydrated mucus. An alternative possibility is that the cilia are compressed toward the epithelial surface (Fig. 6B). To distinguish between these two possibilities, we used bright-field microscopy of HBE cultures mounted in profile to directly measure the maximal height of the cilia during the exposure to solutions of varying osmotic moduli. Large dextran ($d > 50$ nm) or agarose ($d \approx 44$ nm) solutions with osmotic moduli $K < 800$ Pa had negligible effects on the height of the cilia (Fig. 6C and points to the left of the highlighted zone in Fig. 6E). However, cilia height decreased substantially with increasing solution osmotic moduli (Fig. 6D and points to the right of the highlighted zone in Fig. 6E). The value of 800 Pa represents the minimum osmotic modulus (K_{cc}) required to compress the cilia. With exposure to solutions with $K > K_{cc}$, the cilia still beat within this restricted space but not at their full height. These data, coupled with dye measurements of K_0 (Fig. 4), suggest that, with moderate increases in osmotic modulus of the overlaying polymer layer, for example, between $K_0 = 300$ Pa and $K_{cc} = 800$ Pa, there was compression of the brush toward the cilia. Polymer solutions with higher osmotic moduli caused cilia to collapse. Experiments with HBE mucus (red squares, Fig. 6E) revealed that mucus with osmotic modulus $K = 5700$ Pa, similar to that observed in CF, also produced complete ciliary collapse. On the basis of these data, airway cilia do not exhibit sufficient stiffness to resist osmotic collapse during severe airway surface dehydration (supplementary text).

The interface between the mucus layer and the PCL brush is semipermeable. Thus, only the large macromolecules that cannot penetrate the mesh of the opposing layer, and not the freely permeant salts and small globular proteins, generate the "partial" osmotic pressures and moduli that govern water distribution between the two layers. To test this prediction, we exposed HBE cultures to luminal solutions containing small dextrans ($d \approx 2$ nm) with varying concentrations and thus "total" osmotic moduli. These small dextrans freely enter into the PCL and hence are predicted not to produce osmotic compression of the PCL brush. Indeed, no changes in the cilia height were observed, even for solutions of small dextrans producing osmotic moduli exceeding 10,000 Pa (black open circles, Fig. 6E). On the basis of these findings, we conclude that the large macromolecules in the mucus layer (e.g., secreted mucins that cannot penetrate the PCL) are the "partially" osmotically active molecules with respect to the PCL brush.

Conclusion. The gel-on-brush model postulates that the densely tethered macromolecules occupy the periciliary layer, stabilizing the two-layer mucus clearance system by preventing mucus from penetrating the interciliary space. The PCL brush controls the distribution of water between the two layers required for normal mucus clearance. For example, the gel-on-brush model predicts that the normal mucus layer, with a partial osmotic modulus (~200 Pa) lower than the minimal modulus of the PCL ($K_0 \approx 300$ Pa), acts as a reservoir for water in healthy airways, ensuring efficient clearance over a range of airway surface dehydration states (*10*). If the airway surface is sufficiently dehydrated that the partial osmotic modulus of the mucus layer exceeds K_0, the mucus layer compresses the PCL brush and cilia, slowing down and eventually stopping mucus clearance observed in disease, for example, CF (*7*). The resulting immobile mucus forms a nidus for inflammation and bacterial infections (*40*, *41*), leading to chronic lung disease associated with CF and COPD. The increase in the partial osmotic modulus of the mucus layer can reflect either a decrease in the amount of solvent (water), as in CF (*7*), or an increase in amount of secreted mucins as in COPD (*6*). Therefore, the gel-on-brush model has the capacity to unify the pathogenesis of human airway diseases that have in common mucus stasis, inflammation, and infection.

References and Notes

1. J. V. Fahy, B. F. Dickey, *N. Engl. J. Med.* **363**, 2233 (2010).
2. P. M. Quinton, *Physiol. Rev.* **79** (suppl.), S3 (1999).
3. J. J. Wine, N. S. Joo, *Proc. Am. Thorac. Soc.* **1**, 47 (2004).
4. M. Kaliner, Z. Marom, C. Patow, J. Shelhamer, *J. Allergy Clin. Immunol.* **73**, 318 (1984).
5. M. R. Knowles, R. C. Boucher, *J. Clin. Investig.* **109**, 571 (2002).
6. J. C. Hogg *et al.*, *N. Engl. J. Med.* **350**, 2645 (2004).
7. R. C. Boucher, *Annu. Rev. Med.* **58**, 157 (2007).
8. R. Tarran *et al.*, *Mol. Cell* **8**, 149 (2001).
9. L. A. Clunes *et al.*, *FASEB J.* **26**, 533 (2012).
10. R. Tarran, *Proc. Am. Thorac. Soc.* **1**, 42 (2004).
11. M. Mall, B. R. Grubb, J. R. Harkema, W. K. O'Neal, R. C. Boucher, *Nat. Med.* **10**, 487 (2004).
12. H. Matsui *et al.*, *Proc. Natl. Acad. Sci. U.S.A.* **103**, 18131 (2006).
13. R. C. Boucher, *Eur. Respir. J.* **23**, 146 (2004).
14. A. Wanner, M. Salathé, T. G. O'Riordan, *Am. J. Respir. Crit. Care Med.* **154**, 1868 (1996).
15. A. M. Lucas, L. C. Douglas, *Arch. Otolaryngol.* **20**, 518 (1934).
16. E. Houtmeyers, R. Gosselink, G. Gayan-Ramirez, M. Decramer, *Eur. Respir. J.* **13**, 1177 (1999).
17. H. Kalhoff, *Eur. J. Clin. Nutr.* **57** (suppl. 2), S81 (2003).
18. D. J. Smith, E. A. Gaffney, J. R. Blake, *Bull. Math. Biol.* **69**, 817 (2007).
19. J. Iravani, A. Van As, *J. Pathol.* **106**, 81 (1972).
20. A. C. Hilding, *Minn. Med.* **50**, 915 (1967).
21. M. C. Rose, *Am. J. Physiol.* **263**, L413 (1992).
22. C. Wickström, J. R. Davies, G. V. Eriksen, E. C. I. Veerman, I. Carlstedt, *Biochem. J.* **334**, 685 (1998).
23. D. J. Thornton, K. Rousseau, M. A. McGuckin, *Annu. Rev. Physiol.* **70**, 459 (2008).
24. M. Kesimer, A. M. Makhov, J. D. Griffith, P. Verdugo, J. K. Sheehan, *Am. J. Physiol. Lung Cell. Mol. Physiol.* **298**, L15 (2010).
25. H. W. Hovenberg, J. R. Davies, I. Carlstedt, *Biochem. J.* **318**, 319 (1996).
26. J. K. Sheehan *et al.*, *Biochem. J.* **347**, 37 (2000).
27. B. D. Raynal, T. E. Hardingham, D. J. Thornton, J. K. Sheehan, *Biochem. J.* **362**, 289 (2002).
28. J. H. Widdicombe, J. G. Widdicombe, *Respir. Physiol.* **99**, 3 (1995).
29. C. L. Hattrup, S. J. Gendler, *Annu. Rev. Physiol.* **70**, 431 (2008).
30. W. E. Finkbeiner *et al.*, *Am. J. Physiol. Lung Cell. Mol. Physiol.* **301**, L402 (2011).
31. M. E. Monzon, S. M. Casalino-Matsuda, R. M. Forteza, *Am. J. Respir. Cell Mol. Biol.* **34**, 135 (2006).
32. M. Rubinstein, R. H. Colby, *Polymer Physics* (Oxford Univ. Press, Oxford, 2003).
33. G. B. Arfken, H. J. Weber, *Mathematical Methods for Physicists* (Elsevier, Boston, ed. 6, 2005).
34. R. Tarran, B. R. Grubb, J. T. Gatzy, C. W. Davis, R. C. Boucher, *J. Gen. Physiol.* **118**, 223 (2001).
35. A. J. Zuckerman, J. E. Banatvala, J. R. Pattison, *Principles and Practice of Clinical Virology* (Wiley, Chichester, UK, ed. 4, 2000).
36. S. K. Lai, Y. Y. Wang, J. Hanes, *Adv. Drug Deliv. Rev.* **61**, 158 (2009).
37. M. P. Kinsky, S. M. Milner, B. Button, M. A. Dubick, G. C. Kramer, *J. Trauma Inj. Infect. Crit. Care* **49**, 844 (2000).
38. Materials and methods are available as supplementary materials on *Science* Online.
39. L. W. Matthews, S. Spector, J. Lemm, J. L. Potter, *Am. Rev. Respir. Dis.* **88**, 199 (1963).
40. R. S. Baltimore, C. D. Christie, G. J. Smith, *Am. Rev. Respir. Dis.* **140**, 1650 (1989).
41. D. Worlitzsch *et al.*, *J. Clin. Investig.* **109**, 317 (2002).
42. U. Schwab *et al.*, *Infect. Immun.* **70**, 4547 (2002).
43. B. Jachimska, M. Wasilewska, Z. Adamczyk, *Langmuir* **24**, 6866 (2008).
44. S. K. Lai *et al.*, *Proc. Natl. Acad. Sci. U.S.A.* **104**, 1482 (2007).
45. B. C. Tang *et al.*, *Proc. Natl. Acad. Sci. U.S.A.* **106**, 19268 (2009).
46. J. H. Raphael, D. A. Selwyn, S. D. Mottram, J. A. Langton, C. O. O'Callaghan, *Br. J. Anaesth.* **76**, 116 (1996).

Acknowledgments: Funding for this work was provided by Cystic Fibrosis Foundation grants BUTTON07XX0 (to B.B.), BUTTON11G0 (to B.B.), RUBIN09XX0 (to M.R.), and R026-CRII (to R.C.B.); NSF grants CHE-0911588, DMR-0907515, DMR-1121107, DMR-1122483, PHY11-25915 (in part), and CBET-0609087 (to M.R.); and NIH grants K01DK080847 (to B.B.), R01HL077546 (in part to M.R.), P50HL107168, P01HL34322, P01HL108808, P01HL110873-01, P50HL107168-01, P30DK065988, HHSN268200900020, and UL1-RR025747 (to R.C.B.), and R01HL103940 (to M.K.). We thank S. Panyukov and E. B. Zhulina for illuminating discussions, L. Brown for graphical and editorial assistance, S. Randell for the human airway epithelial cells, K. Burns for histology assistance, and R. Tarran for use of the Leica SP5 confocal microscope. M.R. conceived the study, and B.B., L.-H.C., R.C.B., and M.R. designed the experiments. B.B. developed experimental approaches for the osmotic pressure measurements and the PCL permeability and osmotic compression experiments. L.-H.C. prepared regents and, along with B.B., performed the PCL permeability and osmotic compression experiments. C.E. conducted the transmission electron microscopy and immunological experiments. M.K., D.B.H., and J.K.S. provided technical assistance in preparing reagents. M.R., L.-H.C., B.B., and R.C.B. discussed and analyzed the results. M.R. and R.C.B. supervised the whole study. B.B., L.-H.C., R.C.B., and M.R. wrote the paper. The authors declare that they have no competing financial interests.

Supplementary Materials

www.sciencemag.org/cgi/content/full/337/6097/937/DC1
Materials and Methods
Supplementary Text
Figs. S1 to S5
Table S1
References (*47*–*62*)

5 April 2012; accepted 22 June 2012
10.1126/science.1223012